Available online at www.sciencedirect.com
SCIENCE DIRECT®
Surface Science 572 (2004) 103–114
SURFACE SCIENCE
www.elsevier.com/locate/susc

The surface structure of $Fe_3O_4(1\,1\,1)$ films as studied by CO adsorption

C. Lemire [a], R. Meyer [a], V.E. Henrich [b], Sh. Shaikhutdinov [a,*], H.-J. Freund [a]

[a] *Department of Chemical Physics, Fritz-Haber-Institut der Max-Planck-Gesellschaft, Faradayweg 4-6, 14195 Berlin, Germany*
[b] *Department of Applied Physics, Yale University, P.O. Box 208284, New Haven, CT, USA*

Received 11 May 2004; accepted for publication 9 August 2004
Available online 11 September 2004

Abstract

We have studied adsorption of CO on $Fe_3O_4(1\,1\,1)$ films grown on a Pt(1 1 1) substrate by temperature programmed desorption (TPD), infrared reflection absorption spectroscopy (IRAS) and high resolution electron energy loss spectroscopy (HREELS). Three adsorption states are observed, from which CO desorbs at ~110, 180, and 230 K. CO adsorbed in these states exhibits stretching frequencies at ~2115–2140, 2080 and 2207 cm^{-1}, respectively. The adsorption results are discussed in terms of different structural models previously reported. We suggest that the $Fe_3O_4(1\,1\,1)$ surface is terminated by 1/2 ML of iron, with an outermost 1/4 ML consisting of octahedral Fe^{2+} cations situated above an 1/4 ML of tetrahedral Fe^{3+} ions, in agreement with previous theoretical calculations. The most strongly bound CO is assigned to adsorption to Fe^{3+} cations present on the step edges.

Keywords: Iron oxide; Platinum; Carbon monoxide; Water; Thermal desorption; Infrared absorption spectroscopy; Electron energy loss spectroscopy (EELS); Chemisorption; Single crystal surfaces; Surface structure, morphology, roughness, and topography

1. Introduction

Iron oxides are important materials in many technological applications such as heterogeneous catalysis, magnetic recording media, chemical sensors, etc. [1,2]. In the last decade, single crystals and epitaxially grown thin films were used as suitable systems for studying the iron oxide surfaces at an atomic level. Most of the studies reported so far have been focused on the structural analysis of the iron oxide surface as studied by low energy electron diffraction (LEED), scanning tunneling microscopy (STM), X-ray photoelectron diffraction (XPD) and electron energy loss spectroscopy (EELS) [3–14]. The *adsorption* properties of iron

* Corresponding author. Tel.: +49 030 8413 4193; fax: +49 030 8413 4101.
E-mail address: shaikhutdinov@fhi-berlin.mpg.de (Sh. Shaikhutdinov).

0039-6028/$ - see front matter © 2004 Elsevier B.V. All rights reserved.
doi:10.1016/j.susc.2004.08.033

oxide surfaces and how they relate to the surface structures have been studied to a lesser extent. Basically, researchers focused on adsorption of water on different surfaces of Fe_3O_4 [15–17] and Fe_2O_3 [18,19]. Weiss and co-workers also studied ethylbenzene and styrene adsorption on different iron oxide films [3,20,21]. Recently, Flynn and co-authors have studied CCl_4 adsorption on a $Fe_3O_4(1\,1\,1)$ surface formed under reducing conditions on an α-$Fe_2O_3(0\,0\,0\,1)$ single crystal [22].

Adsorption studies may be very helpful for understanding the surface structure of oxides. In addition, the knowledge of adsorption properties of oxides is necessary for elucidating mechanisms of catalytic reactions over metal particles deposited on oxides. This issue becomes particularly important for metal catalysts supported on reducible oxides such as hematite and magnetite. However, the chemistry of molecules such as water and hydrocarbons is quite complex, as it may include temperature dependent decomposition processes of the adsorbed molecules. In this context, carbon monoxide is a probe molecule preventing these problems, and its adsorption properties may be directly correlated with the surface structure of oxides. In addition, CO adsorption on many surfaces has been extensively studied both theoretically and experimentally.

In this paper, we focus on adsorption of CO (and to a lesser extent of water) on $Fe_3O_4(1\,1\,1)$ films using temperature programmed desorption (TPD), infrared reflection absorption spectroscopy (IRAS) and high resolution electron energy loss spectroscopy (HREELS). Based on these and previously reported results, we have reconsidered the structure of the magnetite (1 1 1) surface.

2. Experimental

The experiments were performed in an ultra-high vacuum (UHV) chamber (base pressure below 3×10^{-10} mbar) equipped with LEED (Omicron), a differentially pumped quadrupole mass spectrometer (QMS, Hiden Analytical), an IR-spectrometer (Mattson RS-1 FTIR, spectral resolution $2\,cm^{-1}$) and a HREELS spectrometer (Delta 0.5, VSI).

The Pt(1 1 1) crystal was spot welded to two parallel Ta wires used for resistive heating as well as conductive cooling down to 90 K by use of liquid nitrogen. The chromel–alumel thermocouple was spot welded to the back side of the crystal.

Iron (99.99% Goodfellow) was deposited on clean Pt(1 1 1) using an electron-beam assisted evaporator (EFM3, Focus). During evaporation, the crystal was biased in order to prevent metal ions from being accelerated towards the sample surface. The oxidation of the Fe overlayer as well as gas exposures for TPD and IRAS experiments were performed with a calibrated directional gas doser.

After about one monolayer (ML) of iron is evaporated on clean Pt(1 1 1) and oxidized in 10^{-6} mbar O_2 at 1000 K for 2 min, an FeO(1 1 1) film is formed, as evidenced by LEED. This surface is found to be essentially inert towards CO exposure at 90 K as CO was not detected in our TPD and IRAS spectra. By repeated cycles of ~5 ML iron deposition at 90 K and oxidation at 900 K for 5 min, Fe_3O_4 films 5–7 nm in thickness were grown. The final oxidation step was performed at 1000 K. The LEED patterns of the films showed very sharp spots of $Fe_3O_4(1\,1\,1)$ (see Fig. 1a). The morphology of the films was inspected by STM in another UHV chamber, where the films were prepared using the same growth conditions.

Prior to adsorption experiments, the samples were flashed to 800 K in UHV in order to desorb all species that may have adsorbed from the vacuum background. Then CO (99.999%, AGA) and/or H_2O (degassed by freeze-pumping cycles) were exposed at 90 K. For the TPD measurements, the sample was placed ~0.5 mm from the nozzle of the shield of the QMS. The spectra were taken at a heating rate $3\,K\,s^{-1}$ using a feedback temperature controller (Schlichting Instrum.).

The IRAS spectra presented in the paper are divided by the reference spectrum from a clean $Fe_3O_4(1\,1\,1)$ surface flashed to 800 K before adsorption.

The HREELS spectra were measured in a specular geometry at an incidence angle of 60° relative to the surface normal with a primary electron energy 5 eV. The resolution achieved is $\sim 30\,cm^{-1}$.

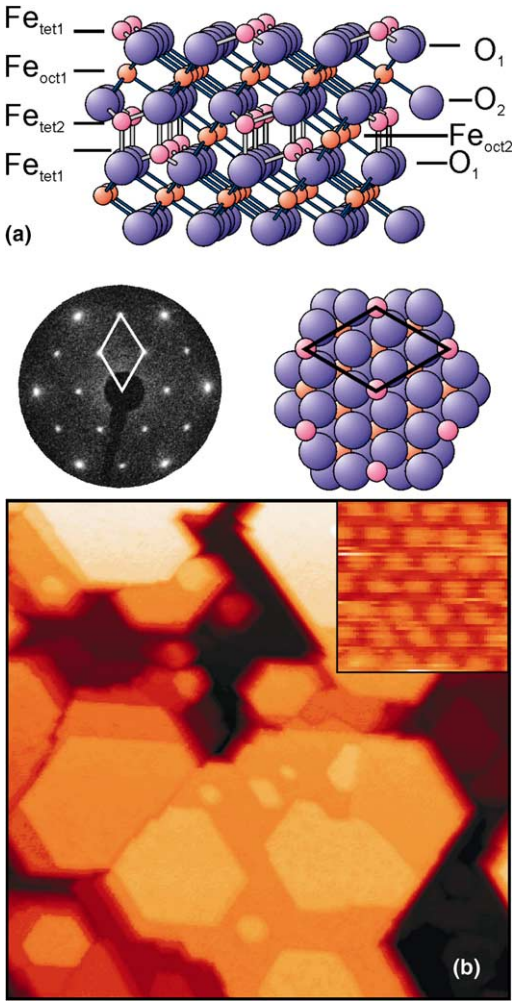

Fig. 1. (a) Side and top view of $Fe_3O_4(1\,1\,1)$. Notation for the layer stacking along [1 1 1] is indicated. The typical LEED pattern at 60 eV for the films grown is shown on the left. (b) Large scale STM image of the $Fe_3O_4(1\,1\,1)$ films (size $300 \times 300\,nm^2$). The inset shows the atomic resolution image (size $3 \times 3\,nm^2$).

3. Results

Fe_3O_4 crystallizes in an inverse spinel structure $[Fe^{3+}]_{tet}[Fe^{2+}Fe^{3+}]_{oct}O_4^{2-}$ where Fe occupies both tetrahedral (tet) and octahedral (oct) sites. As shown in Fig. 1a, the bulk structure of $Fe_3O_4(1\,1\,1)$ consists of close-packed oxygen layers separated by layers of iron in different coordination sites. Therefore, several surface terminations may be formed by cleavage in (1 1 1) orientation.

Fig. 1b shows a typical large scale morphology of the $Fe_3O_4(1\,1\,1)$ films studied, which exhibit terraces separated by steps ~5 Å in height or multiples thereof. This indicates that all terraces are identically terminated, as the distance between identical layers in the bulk is 4.6 Å. The atomic resolution STM images on such films only showed a ~6 Å periodicity as shown in the inset in Fig. 1b.

3.1. CO adsorption

Fig. 2 shows CO TPD and IRAS spectra as a function of CO exposure at 90 K. For each exposure, the IRAS spectrum was recorded first, followed by a TPD run to 600 K. Since the samples were pre-annealed to 800 K prior to the first CO exposure, no morphological changes are expected in the subsequent TPDs. When repeated, both TPD and IRAS spectra were identical; therefore we conclude that the $Fe_3O_4(1\,1\,1)$ films do not suffer from reduction by CO. Indeed, exposure of CO^{16} to the film grown with O^{18} did not result in any desorption signal of $CO^{16}O^{18}$.

At the lowest CO coverage studied, TPD spectra presented in Fig. 2a show two desorption peaks at 150 and 230 K. With increasing exposure, the signal at 230 K gains intensity and saturates at ~0.1 L. Meanwhile, the state at 150 K gradually disappears, and a new state at 200 K emerges which grows and shifts to 180 K from 0.1 to 0.3 L. With further increasing CO coverage, a low temperature state at 110 K is observed. Finally, all states become populated for CO exposures above 1 L. Therefore, TPD spectra show three CO desorption states on the $Fe_3O_4(1\,1\,1)$ surface on saturation, which we refer to as α (at 110 K), β (180 K) and γ (230 K).

The corresponding IRAS spectra are shown in Fig. 2b. At exposures below 0.2 L, two sharp peaks are seen at 2214 and 2098 cm^{-1}, which grow and subsequently saturate with increasing CO exposure. In addition, both signals shift to lower wavenumbers (2207 and 2080 cm^{-1}, respectively), which can be readily explained by an increased CO–CO interaction. Starting from 0.2 L, a small feature is observed at ~2145 cm^{-1}, and a 2112 cm^{-1} shoulder

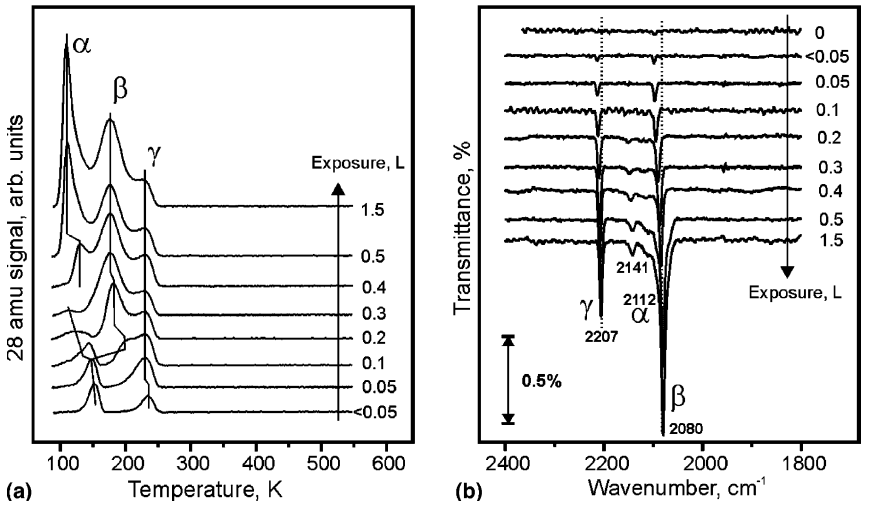

Fig. 2. TPD (a) and IRAS (b) spectra of CO adsorbed at 90 K on the Fe_3O_4(1 1 1) films as a function of CO exposure. Three different states are observed at saturation and labeled as α, β and γ (see the text for details).

emerges at 0.5 L. Therefore, we see that the IRAS peaks correlate well with the α, β and γ desorption signals observed in the TPD spectra at highest coverage.

Fig. 2a shows that α and β peaks seem to develop out of a peak at 150 K observed for the lowest CO exposure. At CO exposure above 0.1 L, the state at 150 K "disproportionates" into less strongly bound and more strongly bound states. Such phase transitions have been observed before in the case of relatively weakly bound systems, e.g. benzene on Ru [23]. The driving force for such a transition is, of course, the minimization of the total energy, which contains both enthalpic and entropic contributions. The α state shows the typical spectral signature of a CO species that is highly mobile on the surface, similar to the CO species observed on Cr_2O_3(0 0 0 1), where the potential energy surface of CO has been investigated theoretically [24]. It is the higher entropy in this state that helps to drive the phase transition, and that allows population of a state of higher binding energy.

Fig. 3a shows the results of temperature programmed IRAS experiments using ^{13}CO. The labeled CO was used in order to diminish the effect of re-adsorption of "normal" ^{12}CO from the vacuum background. The Fe_3O_4 film was exposed to 1.5 L of ^{13}CO at different temperatures and analyzed first by IRAS at the same temperature and then by TPD on heating to 600 K.

At 150 K, we observed five peaks in the IRAS spectrum centered at 2210, 2161, 2103, 2089, and 2044 cm^{-1}. Weak signals at 2210 and 2089 cm^{-1} can be readily assigned to traces of ^{12}CO either present in ^{13}CO as impurity or in the vacuum background. The most intense signals are assigned to adsorbed ^{13}CO (2161, 2103, and 2044 cm^{-1}) analogously to the experiments in Fig. 2b, however the bands are isotopically shifted by ~50 cm^{-1} to lower wavenumbers.

At 165 K, the small peak at 2103 cm^{-1} disappears, and the signal at 2048 cm^{-1} is strongly attenuated relatively to the signal at 2161 cm^{-1}. Finally, by adsorption at 190 K, the only species observed is centered at 2162 cm^{-1}. Fig. 3b shows TPD spectra of mass 29 (^{13}CO) taken after each IRAS spectrum (the traces of ^{12}CO detected by TPD are not shown for clarity).

Therefore, the results clearly demonstrate a good correlation between the species detected in TPD and IRAS. Both Figs. 2 and 3 show that the most strongly bound CO (γ state) is characterized by desorption at 230 K and a CO stretching frequency of 2207 cm^{-1}, while CO desorbs from the β state at 180 K and shows an IR signal at

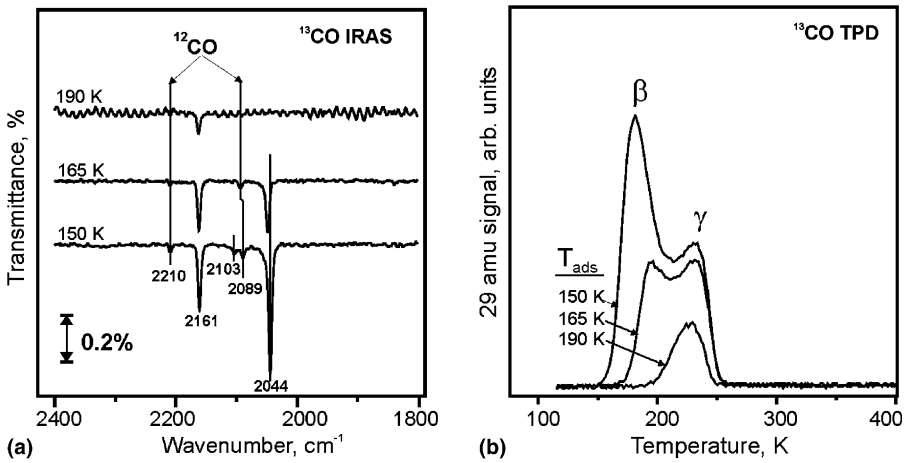

Fig. 3. IRAS (a) and TPD (b) spectra for the $Fe_3O_4(1\,1\,1)$ films exposed to 1.5 L of ^{13}CO at 90 K at different temperatures as indicated.

2080 cm^{-1}. The stretching frequencies of the α species (2140–2115 cm^{-1}) are close to that of CO in the gas phase (2143 cm^{-1}). Therefore, they may be assigned to weakly bound CO desorbing at ~110 K at saturation coverage.

3.2. Effects of water on CO adsorption

Water adsorption was previously studied on similarly prepared $Fe_3O_4(1\,1\,1)$ films. Based on the ultraviolet photoelectron spectroscopy data, the desorption state at ~300 K was attributed to water dissociation on the regular surface of $Fe_3O_4(1\,1\,1)$ [16]. A combined TPD and IRAS study of deuterated water has also shown that D_2O dissociates on $Fe_3O_4(1\,1\,1)$ [17].

In order to see how water affects the adsorption of CO, we have performed H_2O and CO co-adsorption studies on our films using TPD and HREELS.

Fig. 4 shows the TPD spectra of H_2O as a function of exposure at 90 K. At the lowest coverage, a small peak at 380 K is observed. For increasing exposure, several states are subsequently populated until the condensed water film is formed, which desorbs as a sharp peak at ~180 K. These TPD spectra are quite similar to those reported in [16,17], however, the high temperature (HT) state observed in our spectra extends out to

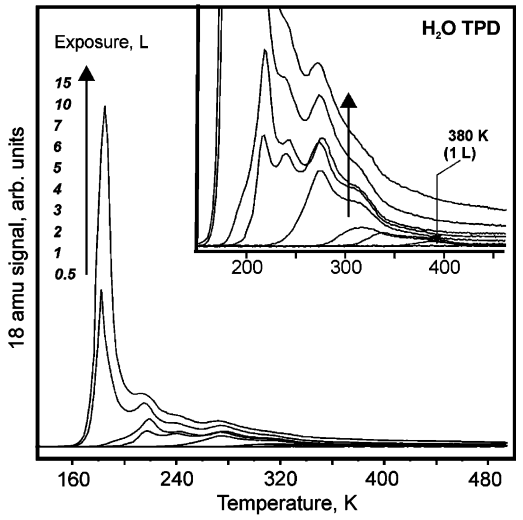

Fig. 4. TPD spectra of H_2O adsorbed at 90 K on $Fe_3O_4(1\,1\,1)$ film as a function of water exposure as indicated. Note the strongly bound state at 380 K detected at the lowest exposure. A condensed layer of water desorbs in a sharp signal at ~180 K.

390 K, which is beyond the ~300 K previously observed.

Fig. 5 shows HREELS spectra of the clean $Fe_3O_4(1\,1\,1)$ film (a), after saturation with 15 L of H_2O at 90 K (b), and subsequent flash to 300 K (c). On the clean surface, four peaks are observed at 115, 265, 415 and 615 cm^{-1} which are consistent

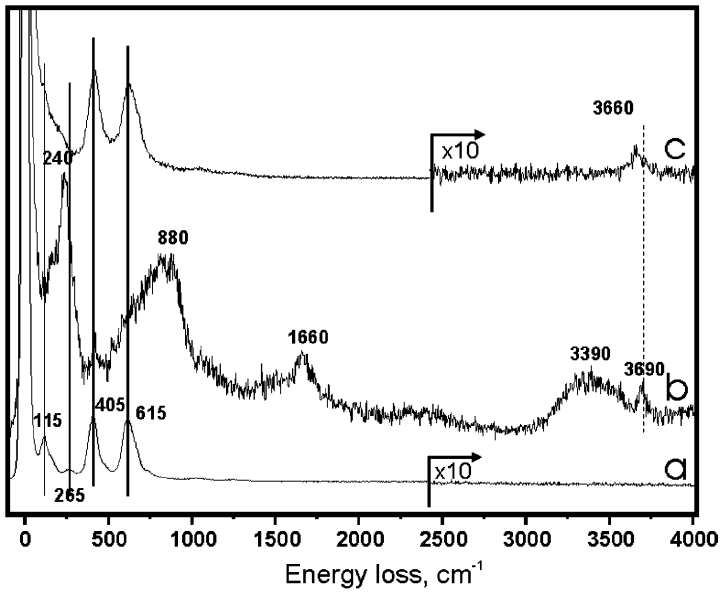

Fig. 5. HREELS spectra of the clean $Fe_3O_4(1\,1\,1)$ film (a), after saturation with 15 L of H_2O at 90 K (b), and subsequent heating to 300 K (c).

with the four IR-active phonon modes predicted theoretically by White and De Angelis [25] and observed by Degiorgi et al. with optical reflectivity measurements [26]. When a condensed layer of H_2O is formed, these phonons are strongly suppressed and new features emerge at 240, 880, 1660, 3390 and 3690 cm^{-1}.

The loss at 3690 cm^{-1} is assigned straightforwardly to a stretching vibration mode of isolated hydroxyl groups, ν(OH) [27]. The relatively broad loss at 3390 cm^{-1} is generally considered to be associated with hydroxyls which have a H bond to neighboring water molecules, $\nu(OH)_H$ [28]. Molecularly adsorbed water manifests itself by the loss at 1660 cm^{-1} assigned to a scissors mode, δ(HOH). The loss at ~880 cm^{-1} can be attributed to vibrational modes, and the peak at 240 cm^{-1} to a frustrated translational mode typical for the ice-like layers [27,28]. After flashing to 300 K, the clean surface is basically restored, and only isolated hydroxyl groups remain adsorbed on the surface.

Our HREELS results support the previously drawn conclusion that water dissociates on $Fe_3O_4(1\,1\,1)$. The presence of hydroxyls on the surface at 300 K, as shown in Fig. 5, suggests that the HT desorption peak at ~380 K observed in TPD spectra results from the associative desorption of dissociated water molecules.

Fig. 6 shows H_2O and CO signals in TPD spectra after the sample was exposed to different amounts of water followed by exposure to 1.5 L of CO at 90 K. Interestingly, the hydroxyl groups formed at the lowest H_2O exposure selectively block CO adsorption in the γ state. This means that water dissociation occurs initially on the same sites where CO adsorbs most strongly. The increasing water exposure gradually inhibits CO adsorption on other sites due to a site blocking effect.

4. Discussion

The combined TPD, IRAS and HREELS results presented above show the presence of three adsorption states of CO on the $Fe_3O_4(1\,1\,1)$ surface, which can be distinguished by desorption temperature and CO stretching frequency: the α state (~110 K, 2140–2115 cm^{-1}); the β state

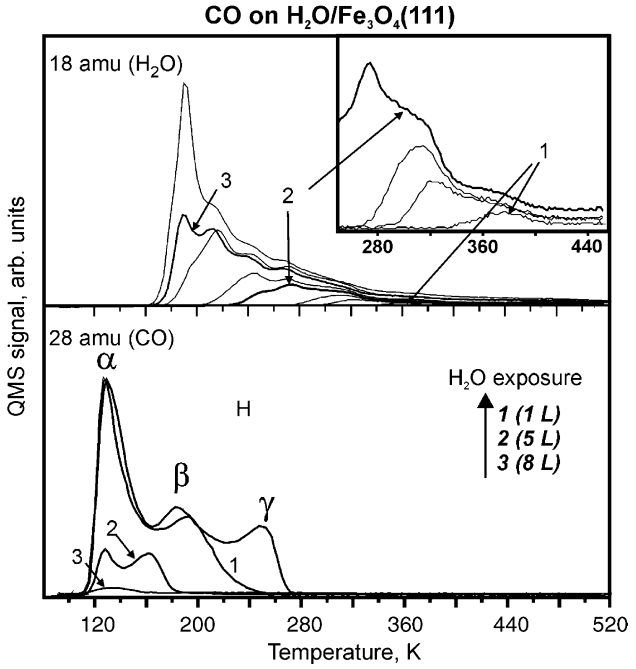

Fig. 6. CO and H_2O signals in TPD spectra of 1.5 L CO adsorbed on the films pre-exposed to different amounts of H_2O at 90 K as indicated. Note that the strongly bound state of water at ~380 K selectively blocks CO adsorption in the γ state.

(~180 K, 2080 cm^{-1}), and the γ state (~230 K, 2207 cm^{-1}). It should be mentioned that we have not observed any other species such as hydroxyls and carbonates on the CO exposed films.

In order to relate the CO adsorption states and the surface structure, we first review the various structural models of the Fe_3O_4(1 1 1) surface previously suggested.

Based on dynamic LEED and STM studies of the Fe_3O_4(1 1 1) films prepared similarly to this study (oxidation at ~1000 K for 5 min in 10^{-6} mbar O_2), Weiss and co-workers have suggested that the surface is terminated by 1/4 ML of Fe^{3+} ions in tetrahedral coordination (Fe_{tet1} in Fig. 1) which form a (2 × 2) structure with respect to the underlying close-packed oxygen layer, which we define as 1 ML. The surface shows a ~6 Å periodicity of protrusions in the STM images [3,9,10], with each protrusions assigned to the Fe cations according to DFT calculations [10]. At low oxidation temperature (ca. 870 K), the film may exhibit small patches of "biphase ordering", where FeO(1 1 1) domains coexist with Fe_3O_4 (1 1 1) in an ordered manner, but they only covered a few percent of the film surface and disappeared at elevated oxidation temperature ~1000 K [10].

Thornton's group studied natural single crystals of Fe_3O_4(1 1 1) cleaned by cycles Ar^+ bombardment and annealing in UHV at 1050 K [6]. Using STM, they observed two coexisting surface terminations. One surface, which dominated after the "oxidative" annealing (at 1173 K for 30 min in 10^{-7} mbar O_2), was assigned to 3/4 ML of Fe_{oct1} atoms and 1/4 ML of O atoms, with each feature arising from a trimer of Fe atoms capped by an O atom, thus also showing a ~6 Å lattice constant in STM. The second surface, whose area increased at the "reducible" annealing conditions (1073 K for 20 min in UHV), was attributed to unreconstructed (1 1 1) termination that exposes the Fe_{oct2}–Fe_{tet1} layers (totally 1/2 ML of iron). Note that the conditions used by Thornton et al. for the surface preparations are much more reducible than those used for preparations of Fe_3O_4 films. Another issue may arise from the preferential sputtering effects during the Ar^+ bombardment of the crystal.

Using LEED, STM and XPD, Salmeron's group studied thin iron oxide films formed on Pt(1 1 1) as a function of thickness of the Fe overlayer deposited prior to oxidation at 980 K for 1 min in 4×10^{-6} mbar O_2 [7]. At the highest coverage studied (3 ML) the film showed a stoichiometry close to Fe_3O_4. Based on XPD results, it was suggested that this surface may be terminated by oxygen as well. However, the LEED patterns of this surface were diffuse and STM images showed that the surface was in fact very rough.

This overview shows that the surface structure of Fe_3O_4(1 1 1) is not well understood. Regarding CO adsorption, there are no systematic studies on CO adsorption on oxides with spinel structure like Fe_3O_4, as pointed out by Zecchina et al. in a review paper [29].

It is generally accepted that CO can be considered as a probe molecule for Lewis acid sites on oxides [30,31]. Owing to the Pauli repulsion between carbon lone-pair electrons and the surface charge distribution, adsorbed CO seems to vibrate against a rigid wall ("wall effect"). As a result, the CO stretching frequency is shifted to higher wavenumbers compared to the gas phase value ($2143\,cm^{-1}$). However, the metal cations which contain fully or partially filled d-orbitals can also interact with the π^*-orbital of CO via an electron back-donation from metal to CO [31]. As a result, the CO stretching frequency decreases. Therefore, the CO stretching frequency is a complex balance of repulsive and bonding contributions.

For iron in the metallic state, CO vibrations are observed in the range between 1530 and $2055\,cm^{-1}$ on various single crystals [32]. Supported Fe catalysts also showed absorption bands at ~1960 and $2020\,cm^{-1}$ typical for linear CO adsorbed on top of the Fe atoms [33]. Therefore, CO species observed here on the Fe_3O_4 films cannot be attributed to metallic iron. In addition, CO desorbs from the iron surfaces at much higher temperatures than 230 K observed in TPD spectra.

Zecchina et al. [34] reported that CO on α-Fe_2O_3 crystallites showed a single IR-feature at $2165\,cm^{-1}$, which the authors assigned to CO bonded to Fe^{3+} ions with only a negligible contribution of the metal–CO back donation effect. Benziger and Larson [33] examined CO adsorption on Fe, FeO and Fe_2O_3 powders. They assigned the absorption bands centered at ca. 1960, 2100 and $2175\,cm^{-1}$ to CO adsorbed on Fe^0, Fe^{2+} and Fe^{3+} sites, respectively.

Based on this information, we can assign the γ state ($2207\,cm^{-1}$) observed in our IRAS spectra to CO adsorbed on the Fe^{3+} cations. Meanwhile, the β state at $2080\,cm^{-1}$ is red shifted as compared to the gas phase, which points to a strong contribution of electron back donation from the d-orbital of iron to the π^*-orbital of CO. In principle, back donation should be enhanced as iron reaches the metallic state. Davydov, reviewing IR data for CO absorption on various oxides [31], has found that that reduction of a valence state typically decreases CO stretching frequencies by $\sim 100\,cm^{-1}$ per one valence. Therefore, we can assign the β state (which is red-shifted by $\sim 120\,cm^{-1}$ with respect to the Fe^{3+} state) to CO adsorbed on Fe^{2+} cations. Accordingly, the α state can be attributed to a weakly bound CO, which in fact shows a lower intensity in IRAS, thus indicating that these molecules are mobile on the surface.

Now we are in a position to see how the CO adsorption results fit the structural models of the Fe_3O_4(1 1 1) surface. The oxygen-terminated surface must be excluded from the beginning, as the close packed oxygen layer does not adsorb CO. This conclusion is supported by the absence of any TPD and IRAS signals for CO exposed to O-terminated FeO(1 1 1) thin films.

The TPD spectra at CO saturation exposure show that the majority of CO is adsorbed in the β and α states (see Fig. 2). By calibrating the mass-spectrometer on CO/Pt(1 1 1) system, we have determined that the amount of CO adsorbed in the γ state is only ~3% of ML, while in the β state is about 0.2 ML. The latter value is close to a 0.25 ML expected for the model predicting the (2×2) layer of tetrahedrally coordinated Fe atoms on top of the O layer as the most stable surface [3,9,10]. However, the bulk cleavage, considered by Weiss et al. in their LEED analysis of Fe_3O_4(1 1 1) films, implies that the outermost Fe cations should formally possess the charge 3+, while our present results indicate that the regular surface is not Fe^{3+}-terminated and rather exposes iron in the valence state 2+. As LEED is not sen-

sitive to the valence of surface atoms, one could simply suggest that the results on CO adsorption are consistent with the model suggested by the LEED results, whereby the top layer is assigned to a 1/4 ML of Fe^{2+} instead of Fe^{3+}. However, this substitution of Fe^{3+} by Fe^{2+} strongly increases excess of the negative charge on the surface and therefore makes the surface unstable. One may argue that the oxide surface should be described within the iono-covalent bond character model. Ritter and Weiss [9] believed that the covalent character is enhanced on the surface, thus resulting in the charge redistribution and stabilizing the surface, which is otherwise unstable within the pure ionic model.

In the following discussion, we stick to the ionic model of the oxide structure description, knowing that this approach has severe limits. In order to fit the CO adsorption results, we begin with considering the terminations exposing Fe^{2+}. According to the bulk structure, the Fe^{2+} ions are only present in the octahedrally coordinated (Fe_{oct1} and Fe_{oct2}) layers, in which half of the ions are present as Fe^{2+} and half as Fe^{3+}. (Note that the electron density is delocalized at temperatures above ~120 K (Verwey transition), which makes magnetite a good conductor. To date, we have no evidence that the metal–dielectric transition induces changes in CO adsorption geometry (see Fig. 3).)

Cleavage between iron sub-layers is the most favorable as it breaks fewer bonds than the cleavage between oxygen and any of the iron layers. Therefore, the surface terminated by Fe_{oct1} is less stable than Fe_{oct2} if there are no additional stabilizing effects present. For example, it was proposed that the surface may be terminated by O-atoms capping trimers of Fe_{oct1} ions and effectively neutralizing the excess of positive charge [6]. However, this model can be excluded as this O-terminated surface would hardly adsorb CO.

Based on STM and surface stability arguments, Thornton's group favored a model with the Fe_{oct2}-termination as the most stable. They showed high resolution STM images which resolved both Fe_{oct2} and underlying Fe_{tet1} atoms [6]. The STM images were very different from those observed in Weiss's [8–10] and our group on numerous films. As mentioned above, the surface was prepared by annealing in UHV after ion sputtering, which may lead to partial reduction of the surface.

The termination of the $Fe_3O_4(1\,1\,1)$ surface was studied theoretically by applying ab initio periodic Hartree–Fock calculations [35]. The calculations confirmed that the surface consisting of two outermost iron layers (Fe_{oct2}–Fe_{tet1}) is the most stable among those arising from an ideal cleavage of bulk. In addition, the authors considered many other models, deviating from the bulk stoichiometry, imposing a symmetry between the layers to cancel the net dipole moment of the entire slab. One of the most stable geometries has been found as Fe_{oct}–Fe_{tet}–O where all octahedral iron cations are in a +2 valence state, and all tetrahedral ions in a +3 state. Moreover, if switching layers is allowed, the calculations showed that Fe_{tet} ions go inward and exchange with the underlying oxygen layer. The main driving force for the permutation is the reduction of the local dipole perpendicular to the surface, but the switch requires overcoming a barrier. It should be mentioned that the authors are aware that the tensor LEED calculations do not match their model well. However, an atomistic simulation of the surface structures of other spinels such as $MgAl_2O_4$ also suggests that stabilization is achieved by terminating the surface in Mg^{2+} rather than Al^{3+} ions [36].

If the surface was terminated by octahedral iron atoms as in the bulk (i.e. consisting of both Fe^{3+} and Fe^{2+} ions within the same layer), we would expect that CO exposed to such surface first adsorbs on Fe^{2+} and then on Fe^{3+}, as the Fe^{2+} ions should adsorb CO stronger as a result of a back donation effect. However, this contradicts the TPD results: the γ (Fe^{3+}) state shows desorption at ~230 K, and the β (Fe^{2+}) state at ~180 K. Moreover, the intensity ratio of desorption signals in TPD spectra from the Fe^{2+} and Fe^{3+} states should be close to 1:1. In contrast, the TPD signal from the γ state is much smaller than β state. Therefore, we conclude, that the outermost layer only consists of Fe^{2+} ions, which is consistent with theoretical calculations of Ahdjoudj et al. mentioned above [35]. This can also explain an observation of a 6 Å periodicity in the STM images by assigning the protrusions to the position of the outermost Fe^{2+} ions, which form a (2×2) lattice with respect to the O

sub-layer. Again, the CO coverage on these sites would be 0.25 ML, which is close to the value ~0.2 ML determined from the TPD analysis of the β state. Finally, applying Finnis's approach [37] on the excess surface charge we have calculated that this model with double Fe layers termination (1/4 ML of Fe^{2+}_{oct} over 1/4 ML on Fe^{3+}_{tet}) has less excess charge than do others.

Regarding the presence of the Fe^{3+} ions on the surface (in the γ state), we associate them with defects rather than the regular surface. Indeed, the TPD results (see Fig. 2) show that the γ state is populated at very low CO exposures (<0.1 L), which is characteristic of adsorption on defects. Finally, water at the lowest coverage selectively blocks CO adsorption in the γ state, which also favors our conclusion since water is generally believed to dissociate on iron oxides initially on defects [14].

In principle, the defect structure may involve iron vacancies. Assuming that the surface stacking sequence is $Fe^{2+}{}_{oct}$–$Fe^{3+}{}_{tet}$–O–···, the vacancy in the top layer could expose Fe^{3+} ions. However, it is unclear why these Fe^{3+} sites would adsorb CO more strongly. Another defect considered on crystalline surfaces is terrace steps, as step edges may also expose iron cations in +3 state. It is generally believed that steps having undercoordinated atoms adsorb molecules more strongly than the terraces. This can explain the higher desorption temperature observed for the γ state. In addition, this can also explain the apparent discrepancy between saturation exposures observed for the γ state in TPD and IRAS spectra. (Indeed, the γ peak in TPD spectra saturates at ~0.1 L while the corresponding signal in the IRAS spectra continuously grows until 0.4 L, see Section 3.1.) At low exposure, CO adsorbing on the steps would be inclined with respect to the terrace normal. As a result, the IRAS peak at ~2207 cm^{-1} is smaller as compared with those standing upright. With increasing population of CO in the β state on the terraces, the latter molecules push CO on the step edges due to repulsive interaction such that CO at the steps stands up normal to the surface, thus increasing the intensity of the IRAS signal.

To the best of our knowledge, the structure of steps on the magnetite surface has not been studied. In order to predict what structures *might* be most probable on step edges, we have considered the concepts of charge neutrality and coordinative unsaturation as generally applied to oxide surfaces.

The observed morphology of $Fe_3O_4(1\,1\,1)$ mostly consists of hexagonal islands (see Fig. 1b); the island edges are in $\{\bar{1}\,1\,0\}$ type directions. In addition, the observed step height of ~5 Å corresponds to two oxygen layers in the crystal structure. The (1 1 1) surface has three-fold rotational symmetry, but it does not possess any reflection planes. Thus hexagonal islands will have two different types of step edges. We refer to the $\{\bar{1}\,1\,0\}$ steps of islands as type A, and the parallel steps on the opposite side of a hexagonal island as type B. About twenty different step structures were considered for $Fe_3O_4(1\,1\,1)$.

To compare the coordinative unsaturation of different step geometries, we calculated the number of dangling bonds (compared to the bulk atom coordination, and summing both cations and anions) in a unit cell of the step, as was done for terraces on Fe_3O_4 in [5,9]. We then weighted the short tetrahedral and longer octahedral bonds in two ways, also following Refs. [5] and [9]. Our criterion for step stability based solely on coordinative unsaturation is having the minimum number of dangling bonds.

In order to compare the amount of excess charge along a step for different step geometries, we applied a method developed by Finnis [37] for determining atomic or charge excesses on surfaces. His approach utilizes a "tapered termination" extending below the surface in order to evaluate excesses in a way that is independent of how many atomic planes of the crystal are considered and independent of any reconstruction and non-stoichiometry in the region of the surface. For steps, we used a tapered termination volume oriented parallel to the surface and extending away from the step into the upper terrace of the step [38]. Three different ionic charge assignments were used: Fe = +8/3, O = −2 [5]; Fe_{tet} = +3, Fe_{oct} = +2.5, O = −2 [9] and, based on the adsorption results reported in this paper, Fe_{tet} = +3, bulk Fe_{oct} = +2.5, surface Fe_{oct} = +2, O = −2. Based solely on ionic charge, the step geometry having

the smallest excess charge per step unit cell was considered to be the most stable. All valence models gave the same relative stability for the steps.

The most stable steps predicted by the two above criteria are shown in Fig. 7. The figure shows that both steps indeed have coordinatively unsaturated tetrahedral Fe ions along the bottom of the step. We believe that these Fe^{3+} cation sites are the observed adsorption sites for strongly bound CO in the γ state on steps on $Fe_3O_4(1\,1\,1)$. Such an analysis does not, of course, predict definitively which step geometry is the thermodynamically most stable one. Full ab initio calculations would be required for that.

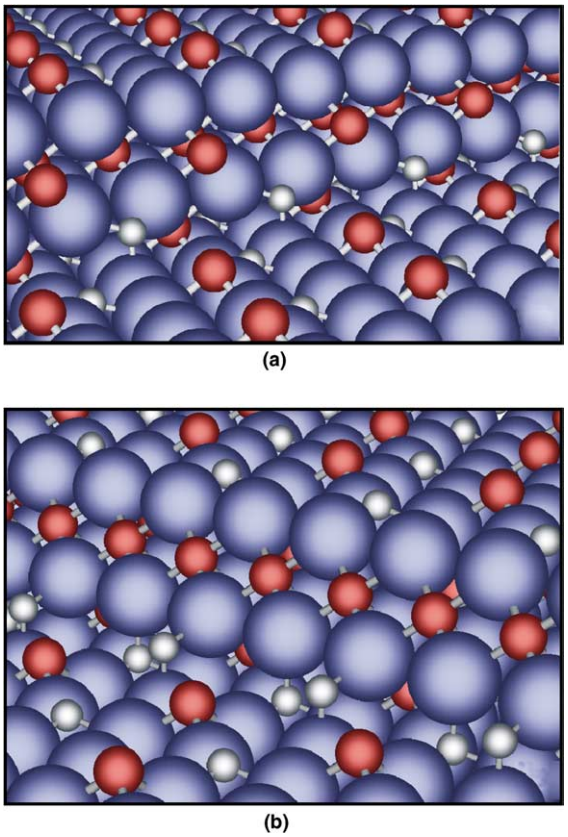

Fig. 7. A-type (a) and B-type (b) steps on $Fe_3O_4(1\,1\,1)$ found as the most stable based on criteria of charge neutrality and coordinative unsaturation. Large blue spheres are O ions, small red spheres are octahedral Fe ions, and smaller white spheres are tetrahedral Fe ions. Ions are shown 80% of their full ionic size.

5. Conclusions

Our combined TPD, IRAS and HREELS study of CO adsorption on $Fe_3O_4(1\,1\,1)$ films grown on a Pt(1 1 1) reveals three adsorption states, from which CO desorbs at ~110 (α), 180 (β), and 230 K (γ). CO adsorbed in these states exhibits stretching frequencies centered at ~2115–2140, 2080 and 2207 cm^{-1}, respectively. The results are discussed in terms of structural models previously reported. We suggest that CO is more strongly bound to Fe^{3+} cations present on step edges (γ state). The β state is assigned to adsorption on regular sites on the terraces, which are terminated by Fe^{2+} cations, in agreement with previous theoretical calculations. Accordingly, the α state is assigned to a weakly bound CO, which shows low intensity in IRAS, thus indicating that these molecules are mobile on the surface.

Acknowledgments

This work was supported by Fonds der Chemischen Industrie. We also acknowledge the EU Training Networks "Catalysis by gold" (AURICAT) and "Reactivity of clean and modified oxide surfaces" (TMR Marseille).

References

[1] J.W. Geus, Appl. Catal. 25 (1986) 313.
[2] J.C. Mallinson, The Foundation of Magnetic Recording, second ed., Academic Press, New York, 1993.
[3] W. Weiss, W. Ranke, Prog. Surf. Sci. 70 (2002) 1.
[4] S.A. Chambers, Surf. Sci. Rep. 39 (2000) 105.
[5] A. Barbieri, W. Weiss, M.A. Van Hove, G.A. Somorjai, Surf. Sci. 302 (1994) 259.
[6] A.R. Lennie, N.G. Condon, F.M. Leibsle, P.W. Murray, G. Thornton, D.J. Vaughan, Phys. Rev. B 53 (1996) 10244.
[7] Y.J. Kim, C. Westphal, R.X. Ynzunza, Z. Wang, H.C. Galloway, M. Salmeron, M.A. Van Hove, C.S. Fadley, Surf. Sci. 416 (1998) 68.
[8] W. Weiss, M. Ritter, Phys. Rev. B 59 (1999) 5201.
[9] M. Ritter, W. Weiss, Surf. Sci. 432 (1999) 81.
[10] Sh.K. Shaikhutdinov, M. Ritter, X.-G. Wang, H. Over, W. Weiss, Phys. Rev. B 60 (1999) 11062.
[11] Sh.K. Shaikhutdinov, W. Weiss, Surf. Sci. 432 (1999) L627.

[12] G. Ketteler, W. Weiss, W. Ranke, Surf. Rev. Lett. 8 (2001) 661.
[13] G. Tarrach, D. Bürgler, T. Schaub, R. Wiesendanger, H.-J. Guntherodt, Surf. Sci. 285 (1993) 1.
[14] T. Kendelewicz, P. Liu, C.S. Doyle, G.E. Brown Jr., E.J. Nelson, S.A. Chambers, Surf. Sci. 453 (2000) 32.
[15] S.A. Chambers, S.A. Joyce, Surf. Sci. 420 (1999) 111.
[16] Y. Joseph, W. Ranke, W. Weiss, J. Phys. Chem. B 104 (2000) 3224.
[17] U. Leist, W. Ranke, K. Al-Shamery, Phys. Chem. Chem. Phys. 5 (2003) 2435.
[18] M.A. Henderson, S.A. Joyce, J.R. Rustad, Surf. Sci. 417 (1998) 66.
[19] M.A. Henderson, Surf. Sci. 515 (2002) 253.
[20] C. Kuhrs, Y. Arita, W. Weiss, W. Ranke, R. Schlögl, Top. Catal. 14 (2001) 111.
[21] Sh.K. Shaikhutdinov, Y. Joseph, C. Kuhrs, W. Ranke, W. Weiss, Faraday Discussions 114 (1999) 363.
[22] K.T. Rim, J.P. Fitts, T. Müller, K. Adib, N. Camillone III, R.M. Osgood, S.A. Joyce, G.W. Flinn, Surf. Sci. 541 (2003) 59.
[23] P. Jakob, D. Menzel, Surf. Sci. 220 (1989) 70.
[24] M. Pykavy, V. Staemmler, O. Seiferth, H.-J. Freund, Surf. Sci. 479 (2001) 11.
[25] B. White, B.A. De Angelis, Spectrochim. Acta A 23 (1967) 985.
[26] L. Degiorgi, I. Blatter-Mörke, P. Wachter, Phys. Rev. B 35 (1987) 5421.
[27] K. Jacobi, K. Bedürftig, Y. Wang, G. Ertl, Surf. Sci. 472 (2001) 9.
[28] M.A. Henderson, Surf. Sci. Rep. 46 (2002) 1.
[29] A. Zecchina, D. Scarano, S. Bordiga, G. Ricchiardi, G. Spoto, F. Geobaldo, Catal. Today 27 (1996) 403.
[30] G. Busca, Catal. Today 41 (1998) 191.
[31] A.A. Davydov, Infrared Spectroscopy of Adsorbed Species on the Surface of Transition Metal Oxides, John Wiley and Sons, 1984, p. 100.
[32] U. Seip, M.C. Tsai, K. Christmann, J. Küppers, G. Ertl, Surf. Sci. 139 (1984) 29.
[33] J.B. Benziger, L.R. Larson, J. Catal. 77 (1982) 550.
[34] A. Zecchina, D. Scarano, A. Reller, J. Chem. Soc., Faraday Trans. 1 84 (1988) 2327.
[35] J. Ahdjoudj, C. Martinsky, C. Minot, M.A. Van Hove, G.A. Somorjai, Surf. Sci. 443 (1999) 133.
[36] M.J. Davies, S.C. Parker, G.W. Watson, J. Mater. Chem. 4 (1994) 813.
[37] M.W. Finnis, Phys. Stat. Sol. A 166 (1998) 397.
[38] V.E. Henrich, Sh.K. Shaikhutdinov, Surf. Sci., submitted.